VORTEX DRAG REDUCTION BY AFT-MOUNTED DIFFUSING VANES

J. E. Hackett†
Lockheed-Georgia Company
Marietta, Georgia

Abstract

A systematic experimental program is described which has lead to a patented vortex diffuser device for drag reduction. This consists of a winglet-like vane mounted from a boom which trails a wing tip. Under C_L-limited conditions on the vanes, it is claimed that the use of an aft location yields greater drag reduction per square foot of vane area and larger-span vanes may be used effectively. There is little interference with the wing tip and adverse effects, such as loss of aileron power after winglet stall, are avoided. It is pointed out that a strong coupling exists between induced drag and wing root bending for near-planar wings. This coupling can be reduced significantly by employing non-planar tips and design flexibility benefits.

1. Introduction

Figure 1 illustrates a long-recognized fact that cross-flow kinetic energy aft of a wing tip represents a substantial portion of aircraft drag at typical cruise speeds and below. Inventions which attempt to tap this source of energy, thereby reducing drag, have appeared in the patent literature at regular intervals for several decades.[1-8] The advent of the Middle-Eastern oil crisis, in the mid '70's, provided a new impetus for drag reduction, and additional devices have been reported.[9-11]

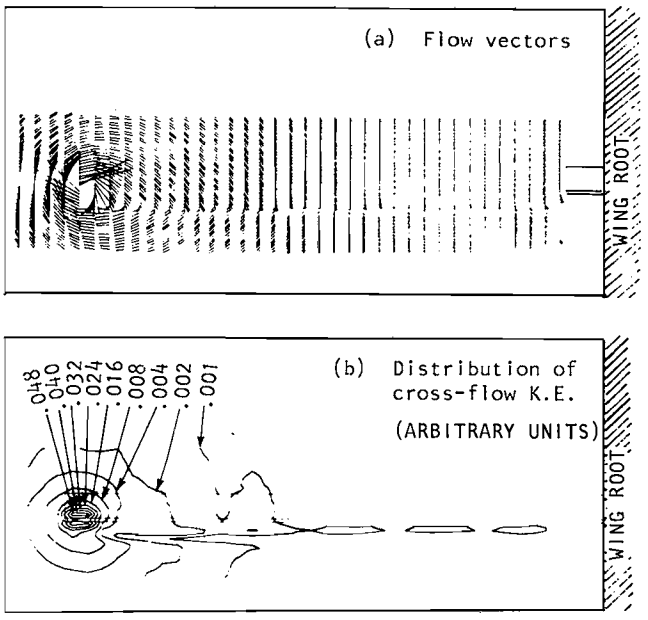

Figure 1. Cross-Flow Vectors and Kinetic Energy Contours Aft of A Simple Wing, $\alpha = 6°$

The present paper summarizes development work, started late in 1973, which has lead to the single-vaned, aft-mounted vortex diffuser device illustrated in Figure 2.[11-14] The earliest work was directed towards vortex hazard alleviation. However, as the realities of the oil situation became apparent, emphasis was shifted towards drag reduction, and this interest continues. Very recently, vortex modification has again become of interest, in connection with aerial spraying operations.

Aft-mounted vanes (Figure 2) have been emphasized throughout the studies described here. The rationale for this location is discussed in Section 2, and flow measurements with some early devices are described. The first balance measurements were made upon a C-141 aircraft model.[13,14] These and subsequent drag reduction experiments upon simpler wings are described in Section 3. Such experiments lead to the development of scaling laws which permit vane performance to be predicted for any configuration for which the span load distribution can be defined (see Section 4). Wing root bending considerations are reviewed in Section 5 and drag/bending moment is discussed. Applications for vortex diffusers are discussed in Section 6 and conclusions are presented in Section 7.

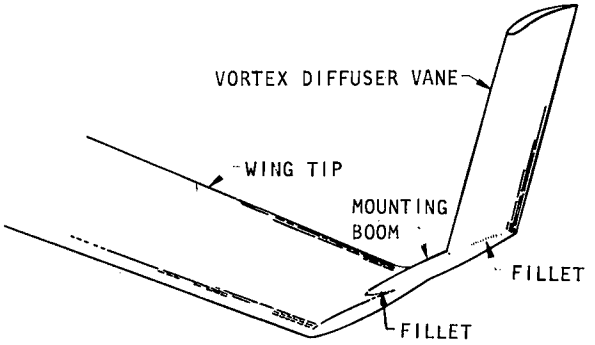

Figure 2. Typical Vortex Diffuser, Single-Vane Installation.

†*Staff Scientist, Advanced Flight Sciences Department.*

2. Development of Concept

2.1 Recovery of Cross-Flow Energy as Thrust

Figure 3 shows a horizontal cross-section of a near-vertical vane similar to the one shown in Figure 2. The trailing vortex system induces inflow and the resultant velocity vector is inclined at an angle α_i to the mainstream direction. The resultant force on an ideal infinite vane in potential flow would be inclined forward by the same angle, but for a real vane there is some reduction – typified by the angle $\cot^{-1}(L/D)$ in Figure 3 – due to finite span and viscous effects. In order to achieve net thrust, α_i must be sufficiently large to overcome these effects, as may be seen from the equation:

$$C_{d_{NET}} = - C_\ell \left[1 + \left(\frac{D}{L}\right)^2\right]^{\frac{1}{2}} \sin\left[\alpha_i - \cot^{-1}\left(\frac{L}{D}\right)\right] \qquad (1)$$

For small angles, this becomes

$$\frac{C_{d_{NET}}}{C_\ell} = - \left[\sin\alpha_i - \left(\frac{D}{L}\right)\cos\alpha_i\right]$$

$$\simeq - \alpha_i + \left(\frac{D}{L}\right) \qquad (2)$$

It is evident that the vane can produce no net thrust if $\alpha_i \leq (D/L)$.

Equation (2) may also be written

$$C_{d_{NET}} = - C_\ell \alpha_i + C_d \qquad (3)$$

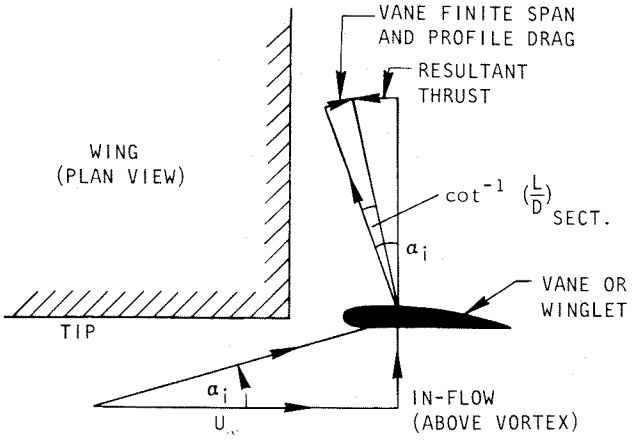

Figure 3. Flow and Force Vectors Near to A Trailing Vortex

2.2 Configuration

Trefftz-plane analyses show that, in potential flow, cross-flow drag depends only upon the distribution of wing or vane loads projected onto a transverse plane and is independent of their axial location.[15,16] However, we shall see below that real flow effects may modify this conclusion and indicate that an aft location could be preferable for devices intended for vortex drag reduction.

Though analysis of the distribution of cross-flow kinetic energy (Figure 1) can give general guidance on vane location and design, resort must be made to experiment to determine the impact of complex viscous effects if the vortex core is penetrated. Early experiments which investigate this are described in subsection 2.3.

Choice of Axial Location. A key aspect of the present work, which distinguishes it from the majority of previous investigations lies in the location of the vortex diffuser in a plane aft of the wing. The rationale for this is based upon a recognition of real flow effects.

It is well recognized that the cross flow, at a given distance from the tip chord line or its extension, increases markedly on proceeding aft from the wing quarter chord location. In an idealized model, the cross flow far downstream is twice that at the quarter chord. A large proportion of this increase is present in a region near to the vortex just aft of the wing trailing edge.

Figure 4 is a plot of Equation (3) for a typical airfoil section, showing net drag as a function of vane sectional lift coefficient for various induced inflow angles α_i (Figure 3). At low values of α_i, the interplay between the first and second terms of Equation (3) leads to an optimum vane C_ℓ for a given α_i. At higher α_i values the optimum shifts strongly towards $C_{\ell_{max}}$ as the effect of the $C_\ell\alpha_i$ term becomes predominant. Because of the risk of stall, a compromise C_ℓ value must obviously be selected and a value of, say, 1.0 might be appropriate unless high lift devices are fitted.

We shall examine the implications of limiting C_ℓ by means of an example. It is assumed that there is a six-degree cross flow at an altitude h above the wing quarter chord line at the tip. A section of vane placed here, having unit C_ℓ, experiences a net sectional thrust coefficient of

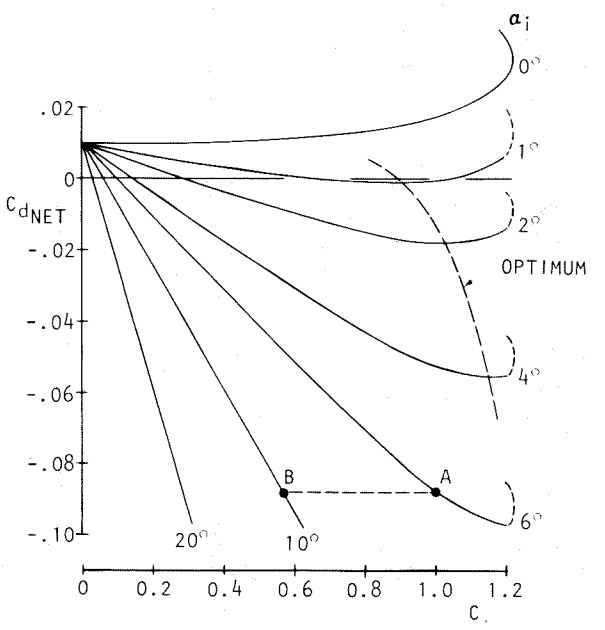

Figure 4. Sectional Drag As A Function of α_i and C_ℓ

0.088 (Point 'A' in Figure 4). If we now consider a corresponding aft location and assume conservatively a 10-degree cross-flow angle, we see that point 'B' gives the same performance. However, the required sectional C_ℓ is now only 0.57. This implies that the sectional chord may be reduced to 57% to its previous value while maintaining the unit C_ℓ criterion. This demonstrates that a shorter-chord, lighter-weight vane may be used at an aft location to achieve a given performance.

The effect of vane setting angle may be illustrated by extending the above example. If the 57% chord vane is now moved from its aft location to the corresponding quarter chord point, its sectional lift coefficient will drop to 0.6, because of reduced cross flow. To restore unit C_ℓ, the vane setting is increased and the vane pressure distribution is as before. However, this loading is directed normally to an α_i vector which is now at 6° rather than the 10° value of the previous aft position. The thrust component therefore has only six tenths of its previous value, even though the total normal load on the vane is the same. This illustrates that the C_ℓ and α_i terms in Equation (3) cannot be traded off once C_ℓ is limited.

Other Benefits. Away from the vortex core, there is a radius beyond which there is insufficient cross flow to balance profile drag. Figure 4 shows that an α_i value of about 1 degree is needed to break even for this particular airfoil section. Following similar reasoning to before, it is evident that more useful thrust can be obtained from the outer regions of the vortex if the vane is aft located. This means that longer, higher-aspect ratio vanes are practical from an aerodynamic standpoint.

In addition to the above performance considerations, further benefits accrue from the aft location. In particular, the geometry assures that the wing flow is affected very little by the vane aerodynamics. This is very important because an on-wing vane stall could trigger tip stall, compromise aileron effectiveness and cause serious roll problems in sideslip. These problems have been demonstrated in in-house experiments at Lockheed-Georgia using a radio-controlled model.

2.3 Flow Measurements

A succession of tests was carried out to determine the general feasibility of aft-mounted vortex diffusers and to investigate the effects of vane geometry. In the earlier tests, observations were limited to three-dimensional flow measurements but, once feasibility was established, force tests were undertaken.

The earliest model, a four-vaned splitter (Figures 5 and 6) was designed essentially as a flow straightener and employed blade entry angles derived from measurements in the vortex. The center was left open in order to avoid low Reynolds number corner flow problems. Figure 7 shows that the device split the vortex into four quite successfully. The residue of the original vortex, which passed through the open center of the device, can also be seen. Because of the coarseness of the experimental grid, no attempt was made to estimate drag reduction from these flow measurements.

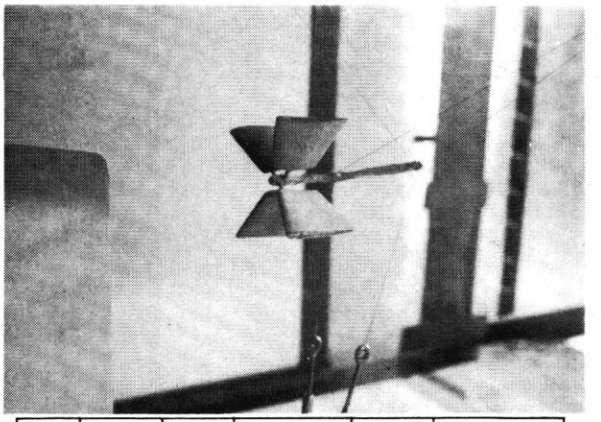

	RADIUS	CHORD	THICKNESS	CAMBER	L.E. ANGLE
ROOT	0.50"	1.50"	15%	24°	19°
TIP	2.50"	2.50"	12%	17°	12°

Figure 5. Details of Four-Vane Vortex Diffuser

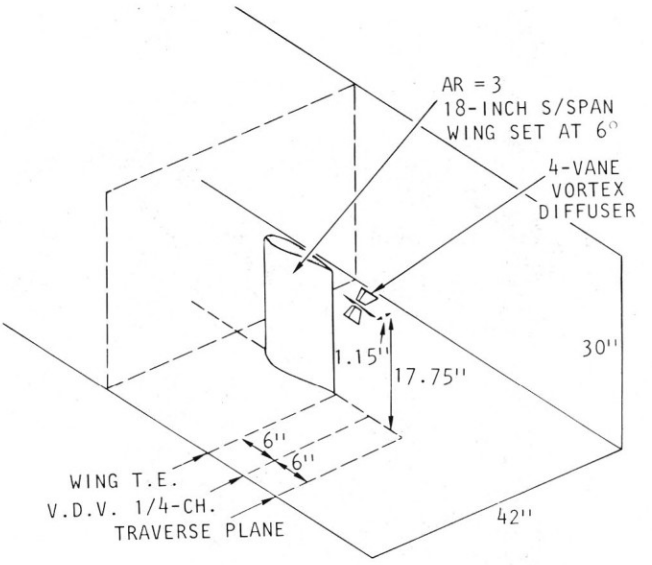

Figure 6. Installation of the Four-Vane Vortex Diffuser

The second model, a larger, aspect ratio two semi-delta, was mounted similarly to the wing in Figure 6 but a 12-inch span two vane, horizontal splitter was employed. Rather than specially tailored, heavily cambered blades, available leading edge slats were used on this model. Figure 8 shows that once again, significant vortex diffusion was achieved and once again a residue of the original vortex can be seen near the splitter center. As the model was larger in relation to the measurement grid, a cross-flow kinetic energy integration was practical (see Figure 9). There is a marked reduction of cross-flow kinetic energy - and hence induced drag - over the splitter span and a slight increase beyond its tips. The net effect was a 19% reduction of cross-flow kinetic energy within the integration boundary. This was the first conclusive proof of the general feasibility of aft-mounted vortex diffusers. Having established this, force tests were needed to examine the trade-offs between potential flow gains (the $C_\ell \alpha_i$ term) and viscous losses (the C_d term) in Equation 3.

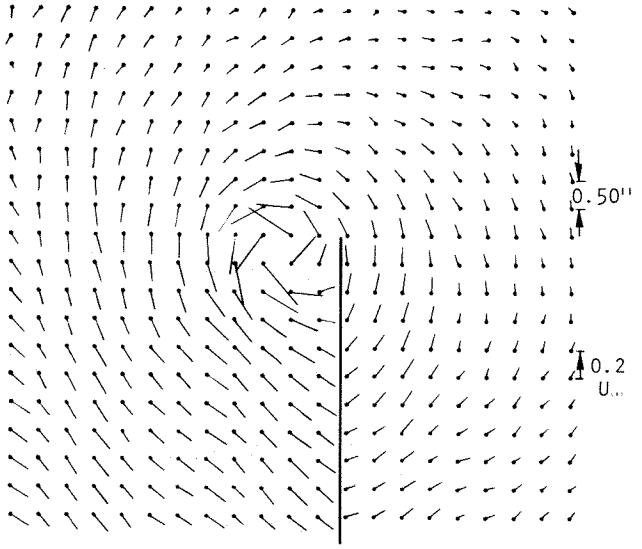

(a) Clean rectangular wing

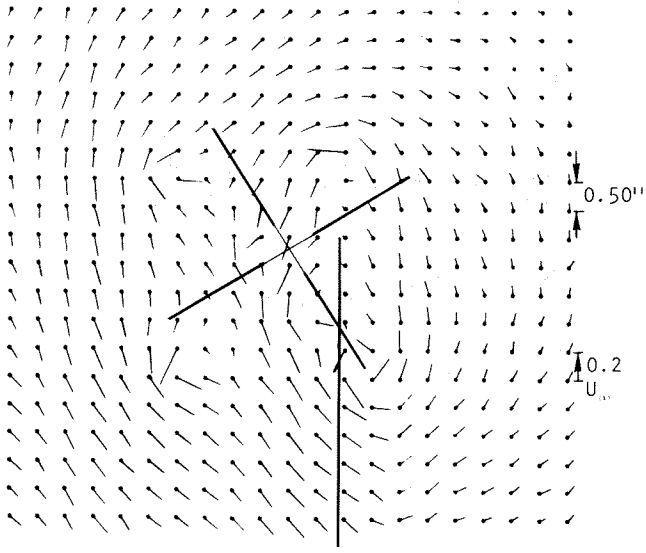

(b) With the four-vane vortex diffuser

Figure 7. Vortex Modification by the Four-Vane Vortex Diffuser, $\alpha_w = 6.0°$

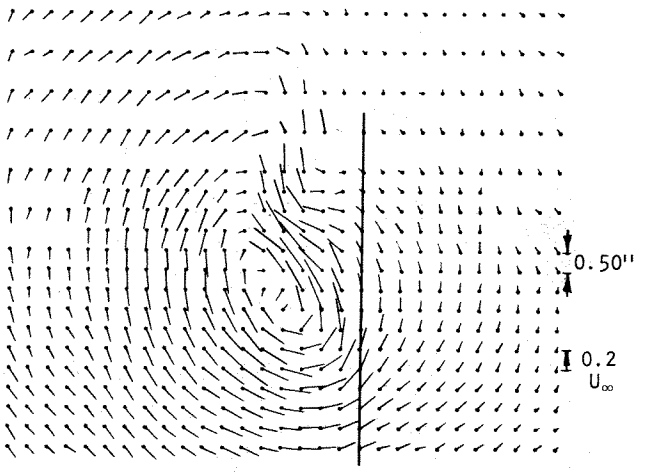

(a) Clean delta wing

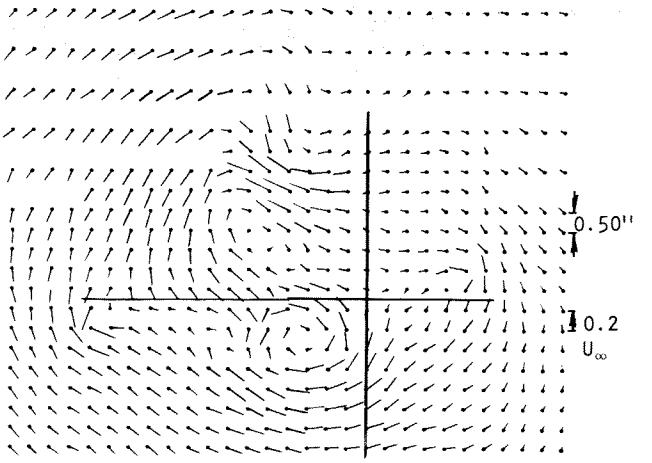

(b) With the two-vane vortex diffuser

Figure 8. Vortex Modification by the Two-Vane Vortex Diffuser, $\alpha_w = 6.0°$

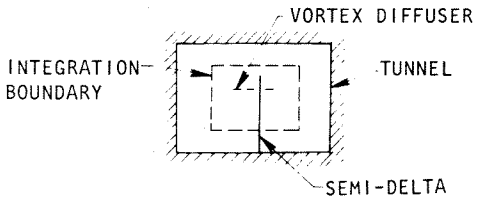

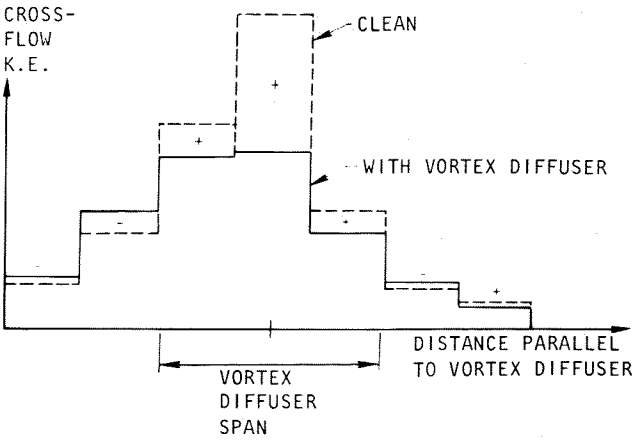

Figure 9. Reduction in Cross-Flow K.E. by the Two-Vane Vortex Diffuser

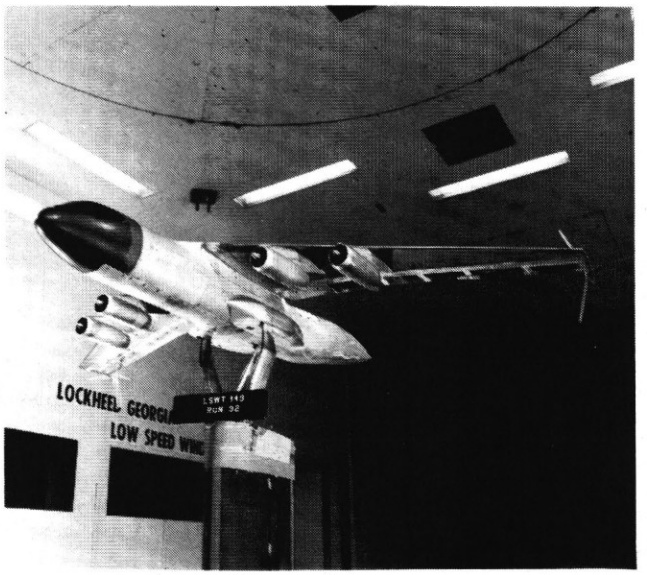

Figure 10. The .044-Scale C-141 Model With Three-Vane Vortex Diffusers Fitted

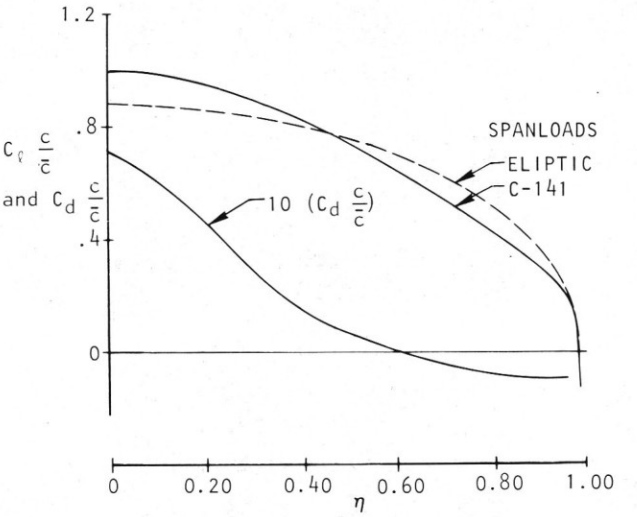

Figure 11. Calculated Span-Load Distribution For the C-141 Model

3. Force Tests

3.1 Tests on a C-141 Model: Three-Vane Diffusers

The initial force tests were carried out as part of a comprehensive drag reduction study for the C-141 transport aircraft (see Figure 10). This aircraft is a poor candidate for wing tip devices because high wing twist and taper give a relatively high root loading and light tip loads (see Figure 11). It is evident that much of the outer wing, which is in an upwash field, experiences thrust.

In view of the above considerations, together with a recognition that low vane chord Reynolds number might be a problem, relatively large vortex diffusers were employed (see Figures 10 and 12). To investigate the relative merits of upward-, downward-, and outward-extending devices, three removable vanes were fitted to each mounting boom. The upper and lower vanes were canted inward by 20 degrees to relieve wing root bending moment. Figure 13 demonstrates how this is achieved for an upward-extending vane. The inward normal force on the upper vane has a downward component which causes the resultant vector to pass below the wing root, thereby reducing the bending moment there. Similarly, a downward and outward force on a canted-in lower vane passes above the wing root, which is again beneficial. The outward-extending vane increases root bending. Wing bending effects will be reviewed further in Section 5.

Initial tests employed the three-vane configuration and drag polars were obtained for nominal vane setting angles, measured positive for nose inboard, from -9.6° to 0°. The sectional zero lift line was streamwise for a -6.4° setting, which turned out to be optimum. Figure 14 shows the basic drag polar together with the envelope polar

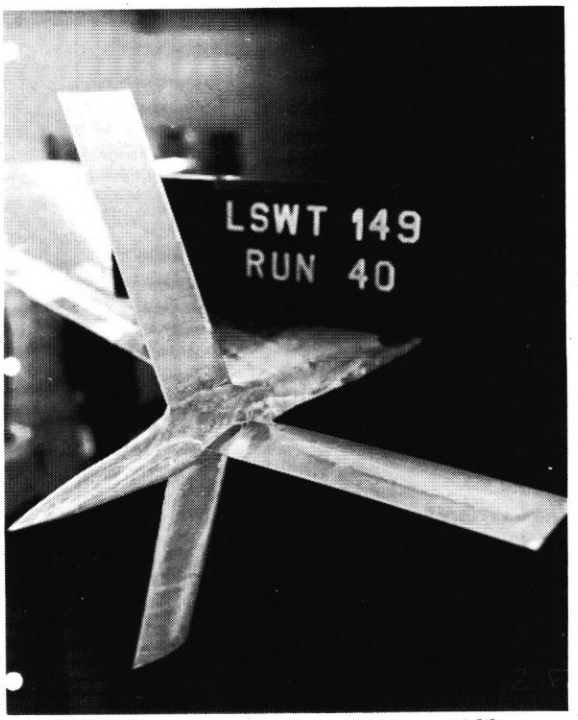

Figure 12. The Three-Vane Vortex Diffuser, Showing Surface Flow

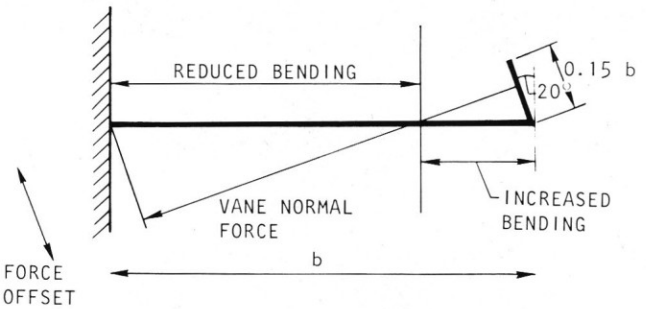

Figure 13. Use of Vane Cant Inward to Reduce Wing Bending at Inboard Locations

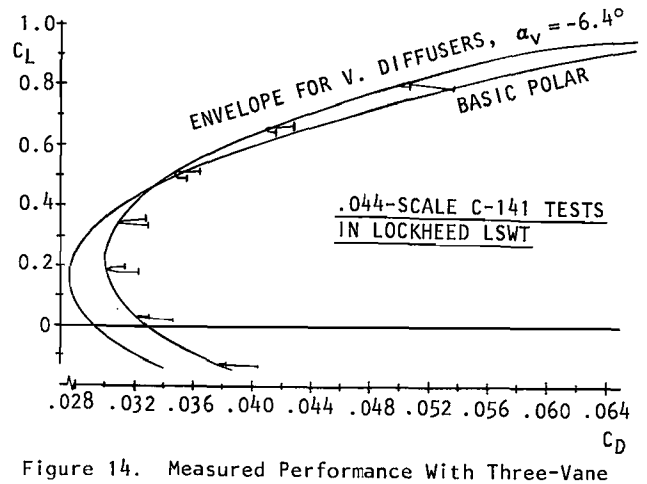

Figure 14. Measured Performance With Three-Vane Vortex Diffuser Fitted

with vortex diffusers fitted. Individual curves are also shown, at given wing angles of attack, which demonstrate the effect of changing the vane setting angles. As setting angle is increased, a slight lift increase is apparent. This is attributable largely to lift on the outward-extending vanes.

As might be expected, there is a substantial profile drag increase at low C_L values, and break-even occurs only when C_L reaches about 0.5 – the cruise value. At higher C_L's decreases in drag become quite substantial. Investigation of vane surface flows (see Figure 12) revealed laminar separation bubbles on upper and/or lower vane surfaces over much of the operating range. The effects of Reynolds number were therefore investigated.

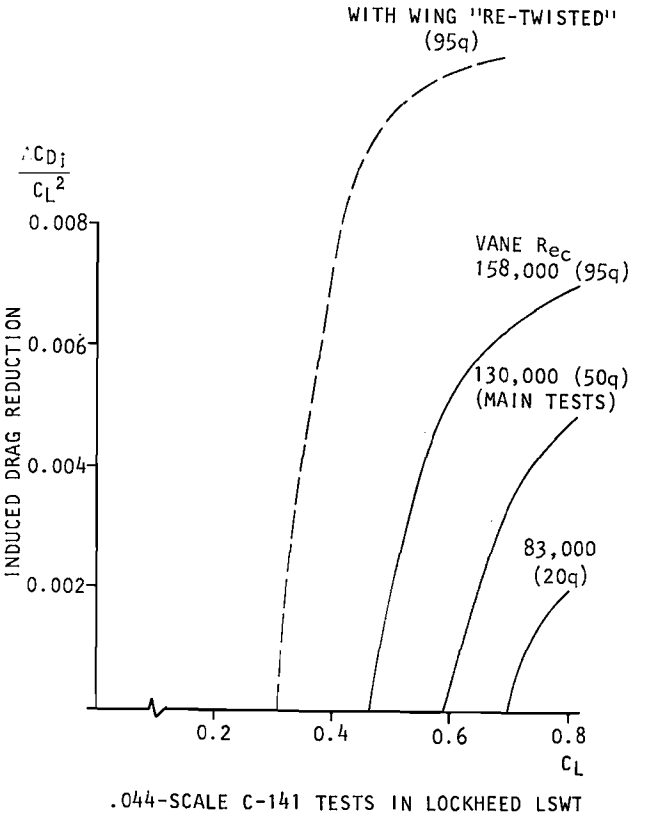

Figure 15. Effects of Reynolds Number and Wing "Retwist"

Figure 15 (full lines) shows the drag reduction obtained, as a function of aircraft C_L, at three test Reynolds numbers. Despite the choice of a section with reputed good low Reynolds number characteristics (St Cyr 244), increase of vane chord Reynolds number from 130,000 to 158,000 produces a dramatic improvement in performance. The results suggest that further increase in Reynolds number would be beneficial. However, tunnel limitations prevented this.

To determine the effect of a fuller tip load distribution, the main wing was modified by adding 10% flat plate trailing-edge extensions which extended from the upper surface of the outer wing and from the lower surface of the inner wing. The broken line in Figure 15 shows that a dramatic improvement in vortex diffuser performance was obtained. This shows that vortex diffusers work better on less heavily twisted wings.

3.2 Effects of Individual Vortex Diffuser Vanes

Having established the feasibility of multi-vaned vortex diffusers by both flow and force measurements, it remained to optimize vane configuration. This was done on the C-141 model by applying the vanes individually and in various combinations, including the use of half-span vanes.

Figure 16 shows a typical buildup from just the mounting spindle to the full, three-vaned configuration. Three aircraft C_L-levels are represented. At low C_L's, the successive addition of components simply adds to drag. At $C_L = 0.5$, favorable cross-flow effects are essentially nullified by profile drag. On the basis of the Figure 15 results, net

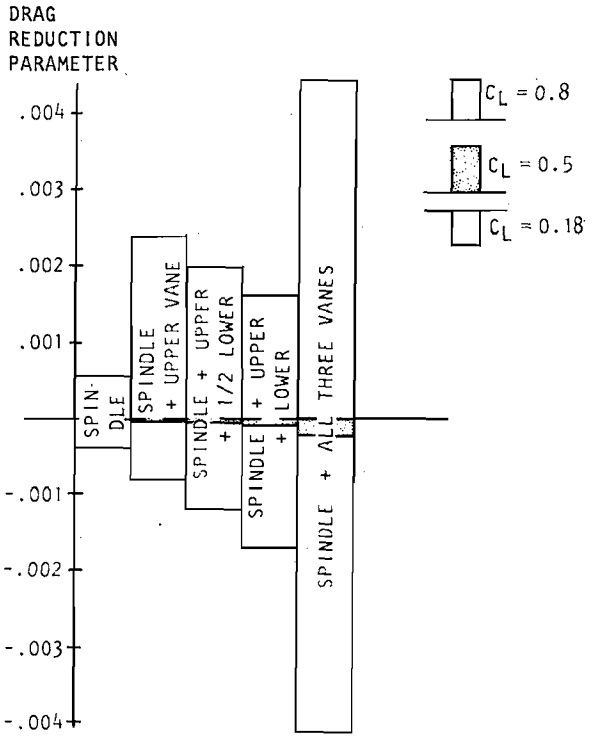

Figure 16. Effects of Individual VDV Components

drag reductions could be substantial, at this C_L, at flight Reynolds numbers and on more tip-loaded wings. However, because of Reynolds number effects in this particular test, it is necessary to consider configuration effects on the basis of $C_L = 0.8$ results. The $C_L = 0.8$ results, on the C-141 wing, are equivalent to results at a lower value of C_L on wings with less twist.

Considering the small geometric change, adding just the vane mounting spindle produces a surprisingly large drag reduction. Adding the upper vane produces a substantial drag reduction but successive drag increases occur on adding first half and then full lower vanes. The addition of the third, outer vane to the other two gives a drag reduction substantially the same as occurred on adding just the upper vane.

Choice of Vane Configuration. The above comparisons show that the upper and outer vane positions are approximately equally effective in reducing drag while the lower position offers no promise. Since the outer position has the disadvantage of increasing wing bending and increasing the spanwise clearance required for aircraft handling on the ground, it is evidently more beneficial and cheaper to use a single, larger area upper vane than to fit both. This line of reasoning together with previous aft-location and bending considertions lead to the configuration shown in Figure 2.

4. Performance Correlation

Because of the vane Reynolds number problems mentioned previously, emphasis was placed initially upon correlations between tested configurations on the basis of wing tip aerodynamic parameters. A major motivation for this was a desire to use partial, wing tip models, with increased vane chord, for development purposes.

4.1 Correlation Between Configurations

As a follow-up to the C-141 model tests, a rectangular 18" semispan wing model was made having the same 5.8-inch tip chord. It was mounted in the same way as the model sketched in Figure 6, but on an accurate platform balance. The same vanes and mounting boom were used as for the C-141 tests.

Figure 17 shows results for the rectangular wing fitted with a single, upper surface vane set at the previous optimum angle, -6.4°. In this, more turbulent smaller tunnel, the vane profile drag was somewhat greater than before. However, the improvement in induced drag factor 'e' on adding vanes is very striking. Tests at other settings showed that the profile drag increments were minimized and the performance benefits were maximized at a vane setting of 0°. Vane-alone measurements (Figure 18, broken line) showed a steep increase in profile drag at negative angles of attack, which explains the large drag increment at zero lift in Figure 17.

In order to determine wing tip loadings for correlation between the C-141 and rectangular wing results, vortex lattice theoretical models were set up for both wings, taking care to ensure that the panel details at the tip were identical. Span load distributions were computed for the two clean wings. Lattice represented diffuser vanes were then added

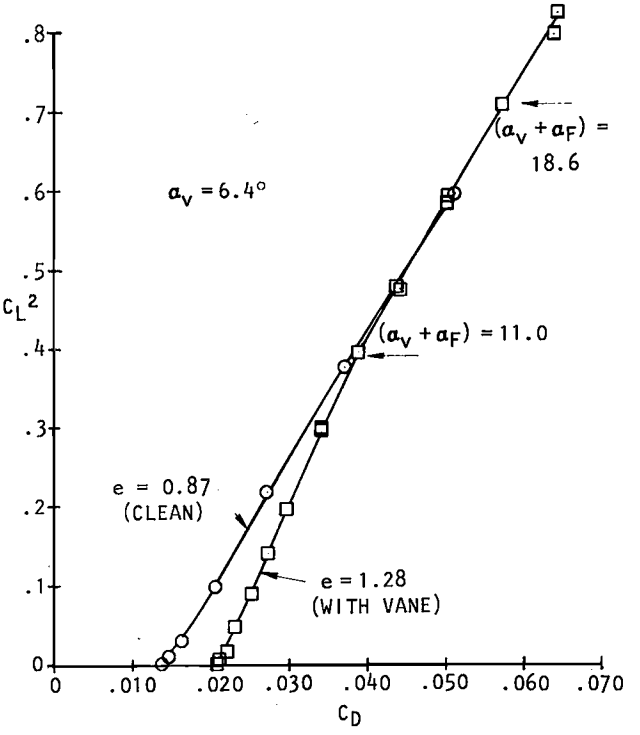

Figure 17. Performance of A Single-Vane VDV Mounted on A Rectangular Wing

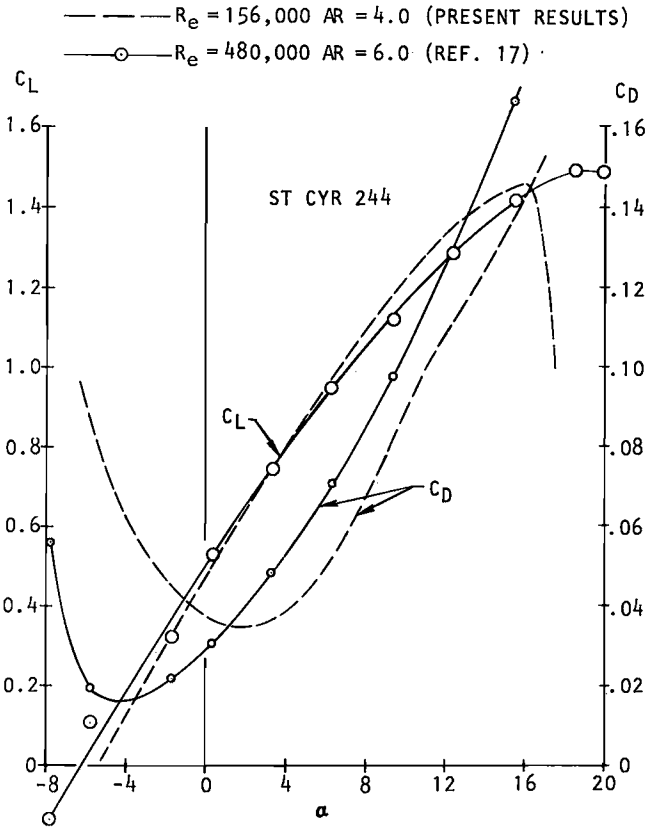

Figure 18. Low Reynolds Number Effects on Airfoil Performance

and their potential flow performance was calculated. This performance was then correlated against various parameters related to the clean wing span load in the vicinity of the tip. The most successful correlation parameter was a lift coefficient derived from the lift carried in a region extending inward from the tip for one tip chord and a reference area equal to tip chord squared. The resulting tip lift coefficient is designated C_{L_T}.

Figure 19 shows optimum performance results for the C-141 and the rectangular wing, correlated using C_{L_T}. In order to make drag results compatible, these are renormalized to a tip chord squared reference area. The results show that partial-tip model tests may be correlated with confidence using C_{L_T} as a correlation parameter.

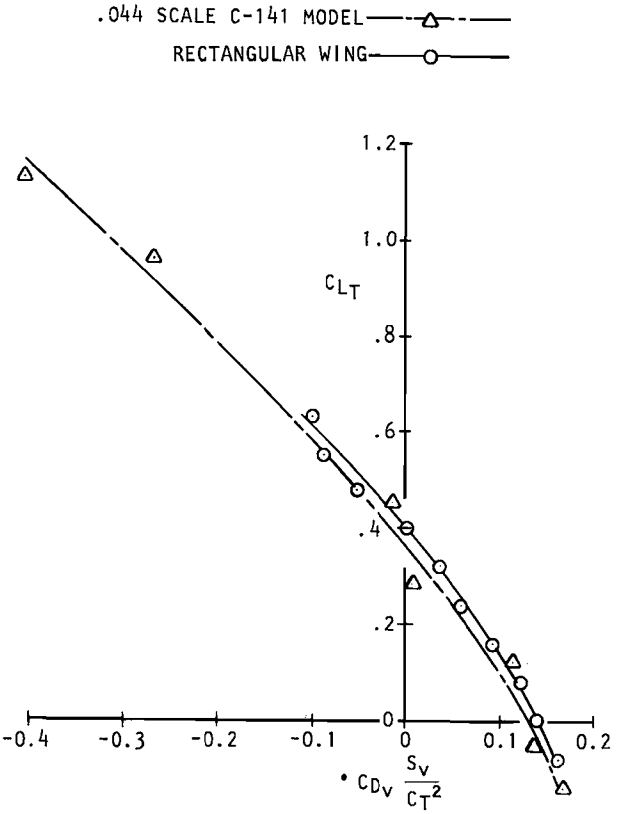

Figure 19. Use of Tip C_L as A Correlation Parameter

4.2 Correlation From Vortex Lattice and Airfoil Properties

The airfoil data shown in Figure 18 (broken line) was obtained with a single, aspect ratio four vane extending outward from the mounting boom, with the main wing set to zero lift. While the data obtained are more credible than those found in Reference 17 (particularly concerning the location of the drag bucket), they must nonetheless be considered largely qualitative because of finite span effects.

Figure 20 shows measured drag or thrust increments for a single-vaned vortex diffuser (points) compared with predictions by two methods (full and broken lines). Both theoretical approaches employed the rectangular-wing-plus-vane vortex lattice potential flow model described above. In the present case, however, the vortex lattice boundary condition comprised measured clean-wing flow vectors. A drag increment was added for skin friction based firstly upon simple, flat plate skin friction (full lines) and then using data from Figure 18 (broken lines). In the latter case, an increment corresponding to mean vane C_L (via vortex lattice) was employed. More detailed predictions, using strip theory for example, were not considered worthwhile.

The correlations in Figure 20 are better than might be expected in the present circumstances. Both the trends and the predicted values agree quite well at vane setting angles of -6.4° and -3.2°. However, the predictions become less accurate as the vane becomes highly loaded.

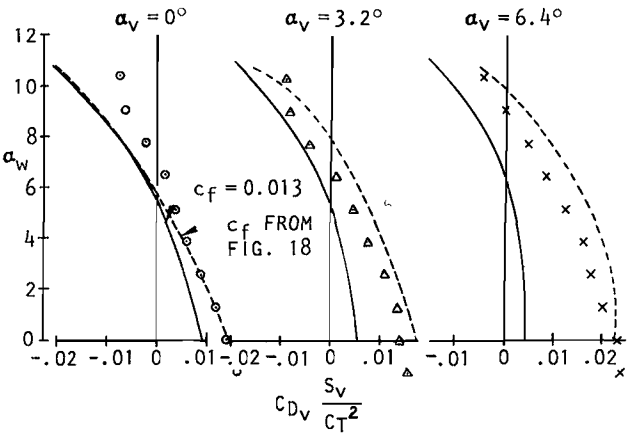

Figure 20. Predicted and Measured Vortex Diffuser Performance

5. Wing Bending Moment

5.1 Introduction

Historically, the aerodynamic and structural design of wings have been essentially independent processes. The aerodynamicist has come to realize that a wing with an aspect ratio between 7 and 10 and a taper ratio of 1/3 to 1/2 can be accepted structurally. He adds twist to the wing to avoid tip stall and designs for an elliptic load distribution at cruise to minimize induced drag. He then hands the details of his wing to the designer, who determines its structure. Though there may be some iteration after this, it would be unusual for the span load shape to be changed much.

In a classical paper, R. T. Jones recognized the need to consider structural implications while minimizing induced drag.(18) Starting with an elliptically loaded wing and keeping lift and root bending moment constant, Jones showed that still lower values of induced drag could be obtained by permitting the span to increase and adopting a more tapered form of the loading curve. More recently, C. J. Wood, et al. carried out a similar analysis involving yachts.(19) They held mast height (i.e. wing span) and rolling moment (wing root bending) constant. In certain cases, maximum sail thrust (wing lift) was obtained with negative load in the outermost region.

The above examples suggest that the historic approach of optimizing first the aerodynamics and then the structure of a new wing is too narrow: it is likely that simultaneous optimization will produce a better design. A comprehensive application study for vortex diffusers would parallel the References 18 and 19 approach. However, the alternative, more expeditious approach is adopted here of considering perturbations to a given conventional design. While the present study may give insight regarding design strategy for modifications, it is recognized that the results have limited relevance to optimization for a new design.

5.2 Relationship Between Induced Drag and Wing Bending Moment

Planar, or Near-Planar Configurations. In Reference 20, Garner develops a correlation between the vortex drag factor K ($\equiv(1/e)$) and the spanwise center of pressure location $\bar{\eta}$ for a wide spectrum of untwisted wing planforms. His correlation equation is

$$K = 1 + (75\pi^2/16)\ (\bar{\eta} - 4/(3\pi))^2 \qquad (4)$$

or

$$K \equiv \frac{\pi AR\ C_{D_i}}{C_L{}^2} = \frac{C_{D_i}}{(C_{D_i})_{ell.}} = 1 + 8.3332\ (\mu - 1)^2 \qquad (5)$$

where μ is root bending moment normalized to the value for elliptic loading at the same lift. The above relationships hold only for relatively simple span load shapes: flapped and "M"-shaped wings, for example, are excluded.

Equation (5) shows that there is a one-to-one relationship between wing root bending and induced drag for simple near-planar planforms. The opportunities for design trades are therefore very restricted.

Nonplanar Configurations. A simple example may be used to show that, on removing the near-planar restriction, the coupling between induced drag and wing root bending moment is relaxed considerably. Compare the performance of a wing having span s and chord c, which carries a lift L, with that of two wings with a large vertical spacing. If each of the two wings has span s, chord (c/2) and carries lift L/2, it is readily shown that their combined drag is half that of the base case while the sum of the two root moments equals the root moment for the base case. If the two wings approach each other, the drag increases but the total root moment is unchanged: there is evidently no coupling in this case. The same result may be derived more fundamentally via an analysis in the Trefftz plane.

Tip devices, such as the vortex diffuser vane, can spread trailing vorticity relatively little compared with the two-wing example quoted above. Nonetheless, a number of differing drag/root-bending relationships appear to be possible. To illustrate this, idealized vortex lattice calculations have been carried out on the configurations sketched in Figure 21. A planar, aspect ratio five rectangular wing is the baseline in all cases and flat plate extensions are added in various ways. Figure 22 shows the corresponding percentage changes in induced drag and root bending. Wetted area was held constant throughout so as to hold profile drag approximately constant. Total lift was also held constant.

The above simple study indicates that the use of nonplanar devices releases the designer from the drag-bending moment coupling implicit in planar configurations [Equation (5)]. It also indicates some potentially favorable effects of aft location and inward vane cant.

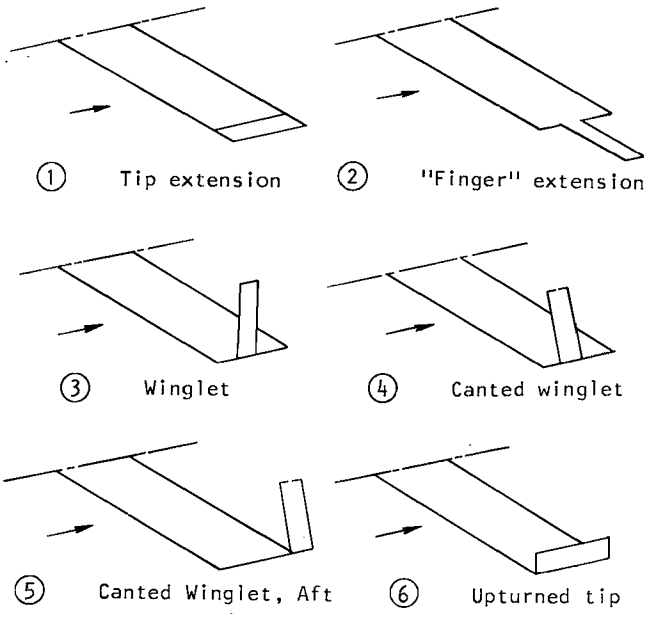

Figure 21. Configurations for Drag/Moment Trade Studies

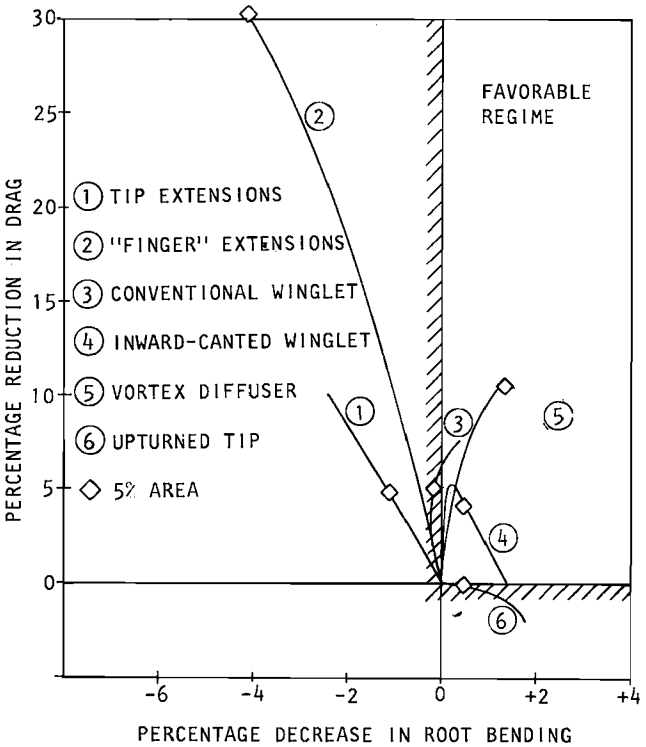

Figure 22. Drag Versus Root Bending Moment Trade for Various Wing Tip Designs

6. Other Applications

The single-vaned vortex diffuser results quoted above and in Reference 14 were correlated using C_{L_T} to give the following prediction formula for a particular vane configuration scaled to tip chord:

$$\Delta C_{D_i} = \text{const} \times C_{L_T}^2 \frac{C_T^2}{S_w} \qquad (6)$$

where C_T is wing tip chord, S_w is wing area and C_{L_T} is the wing tip lift coefficient defined in Section 4.2. To fit the present, low Reynolds number data, a value of 0.16 is assigned to the constant. However, several independent considerations suggest that a value of 0.20 is appropriate when extrapolating to flight Reynolds numbers. This value is employed in what follows.

The geometric and aerodynamic components of Equation (6) are reviewed in Figures 23 and 24, which are taken from Reference 21. The low aspect ratio, constant chord test wings have highly favorable values of C_T^2/S_w. The Caproni glider is included as a counter example, showing that there is little to be gained from a wing of very high aspect ratio. The transport aircraft all fall in a relatively narrow band between these extremes.

The tip lift coefficient, C_{L_T}, in Equation (6), is partly a function of wing planform geometry, but is affected primarily by twist. Because of washout, the tip lifts negatively on most aircraft below C_L of about 0.1 (Figure 24). It is found that C_{L_T} increases with C_L at a constant rate which is about the same for all the transport aircraft studied. It may be seen that the C-5A, the ATA, and the L-1011 have almost the same C_{L_T} characteristics. The C-141 curve, because of high washout, falls well

	SPAN	C_{av}	AR	C_T	C_T^2/S_W	COMMENTS
TEST WINGS						
AR=6 Test Wing	36.00"	5.90"	6.10	5.90"	0.1639	$\lambda = 1$
"Thrush"	40.00"	7.50"	5.33	7.50"	0.1875	$\lambda = 1$
Caproni	67.00"	2.59"	25.87	1.02"	0.0060	Center Wing Const. Chord
TRANSPORT AIRCRAFT						
C-141	84.00"	10.69"	7.90	5.80"	0.0374	Bat
ATA	124.67"	18.10"	6.89	9.50"	0.0400	Bat
L-1011	155.00"	22.30"	6.95	10.25"	0.0304	Bat
KC-135	130.56"	18.63"	7.00	9.33"	0.0358	No Bat
C-5A	219.65"	29.02"	7.56	15.35"	0.0369	Bat

* Model dimensions

Figure 23. Pertinent Dimensions for Vortex Diffuser Candidates

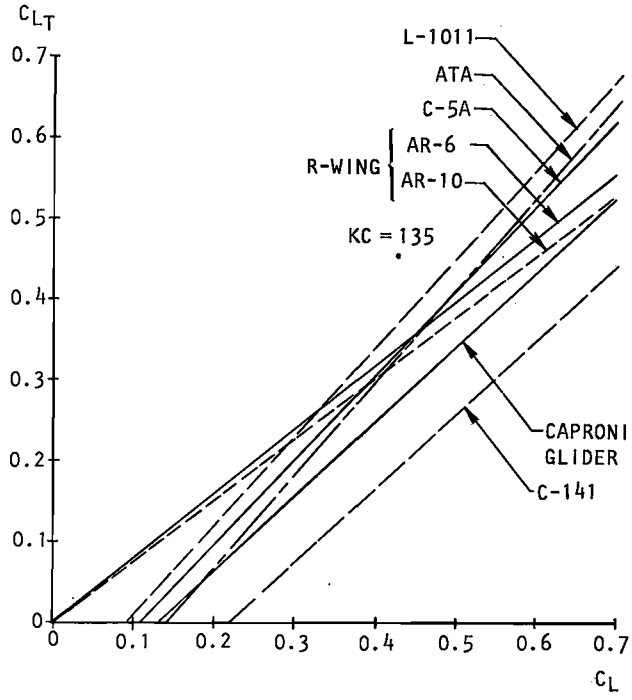

Figure 24. Tip Lift Coefficient, as a Function of C_L, for Various Wings

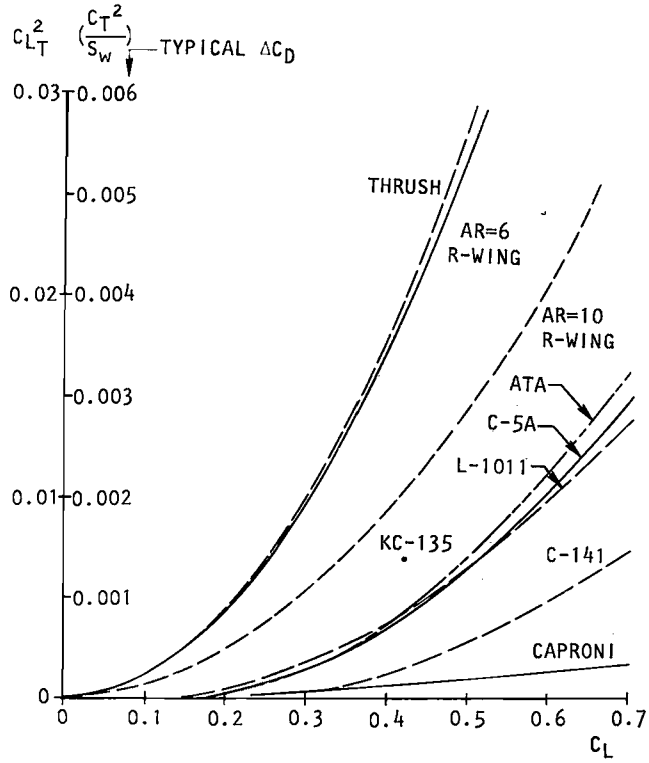

Figure 25. Predictions of Induced Drag Reduction By Vortex Diffusers

below the others. The KC-135 point, derived from Reference 22, indicates that the lack of a bat and possibly less washout have filled out the span-load distribution in a favorable manner. A drag reduction parameter, i.e. the product of C_{L_T} and (C_T^2/S_W), is plotted in Figure 25 together with a ΔC_{D_i} subscale showing estimated reduction in drag coefficient. The C-5A, ATA, and L-1011 are equally good candidates for vortex diffuser application and C-141 is a poor one, for the reasons stated previously.

The KC-135 point is particulary interesting because it provides an opportunity to compare predicted vortex diffuser performance with Boeing's prediction for winglets in Reference 22. The two predictions are almost the same. However, it should be noted that while the winglet is in a highly optimized form, the vortex diffuser technology is at essentially "first-cut" level with regard to vane geometric details.

A major advantage claimed for the vortex diffuser, relative to the winglet and to simple wing tip extension concerns wing root bending. Reference 22, Table 1, shows 4.2% increase in root bending on applying a winglet to the KC-135. These were canted 20 degrees out from the vertical. A corresponding study, using a similarly proportioned vortex diffuser applied to the ATA showed a 4.1% *decrease* in wing root bending.[21] In this case the vane was canted 20 degrees *inward*. It is interesting to note that swinging the same force vector to correspond to 20 degrees outward cant yielded a 5.5% increase in root bending, i.e. comparable to the winglet case. It is not known whether root bending relief due to winglet weight was included in Boeing's estimate. The vortex diffuser therefore presents a benefit in this case, of about 4% relative to the clean wing, 8% relative to a comparable winglet installation and more than 8% for a wing tip extension giving the same performance. The latter may be deduced both from the Boeing paper and from earlier vortex diffuser studies.

7. Conclusions

A systematic development program aimed at reducing induced drag has lead to a vortex diffuser device mounted from a boom which trails the wing tip (see Figure 2). This configuration offers the following advantages:

1. Aft location leads to a device with increased drag reduction per square foot of wetted area under C_L-limited conditions.

2. Larger-span vanes may be used effectively at an aft location.

3. Wing root and inner wing bending moment may be relieved by the use of inward cant.

4. Though a vane extending spanwise is as effective as an upward-extending vane in reducing drag, wing bending considerations favor the latter.

5. Interference with wing tip aerodynamics is minimal for an aft located vane. Problems due to winglet/tip stall in sideslip conditions are therefore largely avoided.

8. Acknowledgements

The work described was carried out under the Lockheed-Georgia independent research and development program. However, opinions expressed are those of the author.

Individual contributions to the work, by the researchers named below, are gratefully acknowledged:

R. A. Boles, for carrying out the experiments

D. E. Lilley, for data handling and flow analysis

V. Lyman, for vortex lattice and performance analysis.

9. References

1. A. W. Loerke, "Wing Tip Vortex Reducer," U.S. Patent No. 2,075,817, April 6, 1937.

2. J.F.G.M.L. Charpentier, "Aeroplane," U.S. Patent No. 2,123,096, March 23, 1936.

3. D. R. Berlin, "Airplane," U.S. Patent No. 2,326,819, August 28, 1940.

4. J. G. Lee, "Rotating Jet Device for Airfoils," U.S. Patent No. 2,477,461, July 29, 1943.

5. E. L. Shaw, "Wing Tip Vortex Reducer for Aircraft," U.S. Patent No. 2,485,218, October 18, 1943.

6. R. Vogt, "Twisted Wing Tip Fin for Airplanes," U.S. Patent No. 2,576,981, February 8, 1949.

7. A. M. Lippisch, "Variable Wing," U.S. Patent No. 2,743,888, October 20, 1951.

8. S. C. Rethorst, "Slotted Diffuser System for Reducing Aircraft Induced Drag," U.S. Patent No. 3,712,564, January 23, 1973.

9. R. T. Whitcomb, "A Design Approach and Selected Wing Tunnel Results at High Subsonic Speeds for Wing-Tip Mounted Winglets," NASA TN D-8260, July 1976.

10. J. J. Spillman, "The Use of Wing Tip Sails to Reduce Vortex Drag," *Aeronautical Journal*, September 1978.

11. J. E. Hackett, "Vortex Diffuser," U.S. Patent No. 4,190,219, February 1980.

12. J. E. Hackett and V. Lyman, "Calculation of Vortex Splitting by a Two-Vaned Dissipator," Lockheed-Georgia Company Engineering Report LG74ER0153, October 1974.

13. J. E. Hackett, "An Analysis of Wing Tip Vortex Diffuser Aerodynamics with Particular Reference to C-141 Application," Lockheed-Georgia Company Engineering Report LG75ER0136, October 1975.

14. J. E. Hackett and V. Lyman, "The Wing Tip Vortex Diffuser: A Review of Drag Reduction Experiments and Analysis at Lockheed-Georgia," Lockheed-Georgia Company Engineering Report LG77ER0234, December 1977.

15. Munk, Max. M., "The Minimum Induced Drag of Airfoils," NACA Report No. 121, 1921.

16. J. A. Blackwell, "A Finite-Step Method for Calculation of Theoretical Load Distributions for Arbitrary Lifting - Surface Arrangements at Subsonic Speeds," NASA TN D-5335, July 1969.

17. Warner and Johnson, *Aviation Handbook.*

18. R. T. Jones, "The Spanwise Distribution of Lift for Minimum Induced Drag of Wings Having a Given Lift and a Given Bending Moment." NACA TN 2249.

19. C. J. Wood and S. H. Tau, "Towards an Optimum Yacht Sail," *J. Fluid Mech.* (1978), vol. 85, part 3.

20. H. C. Garner, "Some Remarks on Vortex Drag and Its Spanwise Distribution in Incompressible Flow." *The Aeronautical Journal of the Royal Aeronautical Society*, July 1968, p. 623.

21. J. E. Hackett and V. Lyman, "Vortex Diffuser Applications." Lockheed-Georgia Company Interdepartmental Communication, E-74-113-78, February 1978.

22. K. K. Ishimitsu, et al., "Design and Analysis of Winglets for Military Aircraft," AFFDL-TR-76-6, February 1976.